MARCEL DEKKER, INC. • 270 MADISON AVENUE • NEW YORK, NY 10016

DRUG DEVELOPMENT AND INDUSTRIAL PHARMACY
Vol. 28, No. 7, pp. 871–888, 2002

RESEARCH PAPER

Scale-Up and Endpoint Issues of Pharmaceutical Wet Granulation in a V-Type Low Shear Granulator

Tom Chirkot

Patterson-Kelley, Co., 100 Burson Street, East Stroudsburg, Pennsylvania 18301
E-mail: chirkott@patkelco.com

ABSTRACT

A 3^2 factorial experiment is conducted in a 57 liter low shear granulator to evaluate the influence of changes in binder strength and agitator speed on the response variables of granule size, granule morphology, granule density and torque input. Results are compared to previous work in a 2 liter granulator and scale-up issues between the two granulators are addressed.

Key Words: *Wet granulation; Low shear; Scale-up; Single pot processing*

INTRODUCTION

The wet granulation process step in pharmaceutical manufacturing converts a formulation of dissimilar constituents into homogenous, similarly sized clusters. These clusters may then proceed to subsequent processing steps without fear of segregation. Methods employed for wet granulation range from high shear devices that impart considerable energy to the system to less energetic devices that primarily use convective motion to provide mixing.[1] Convective motion may develop through an agitator bar, simple tumbling, or gaseous flow.[2]

The literature is rife with information on high-shear granulation and fluid-bed granulation.[3–25] However, little has been published on a class of low-shear granulators (LSGs) that are primarily perceived as powder mixers. These LSGs provide powder movement through both tumbling and internal agitation. Liquid is added through the agitator bar and exits into a toroidal void space carved out by blades located on a disc assembly (Fig. 1). This method of wet granulations offers attributes that set it apart from high-shear granulators (HSGs) and fluidized-bed granulators (FBGs). Among the attributes are a highly efficient liquid delivery system, intimate liquid/solid contact, and

DOI: 10.1081/DDC-120005633
0363-9045 (Print); 1520-5762 (Online)

www.dekker.com

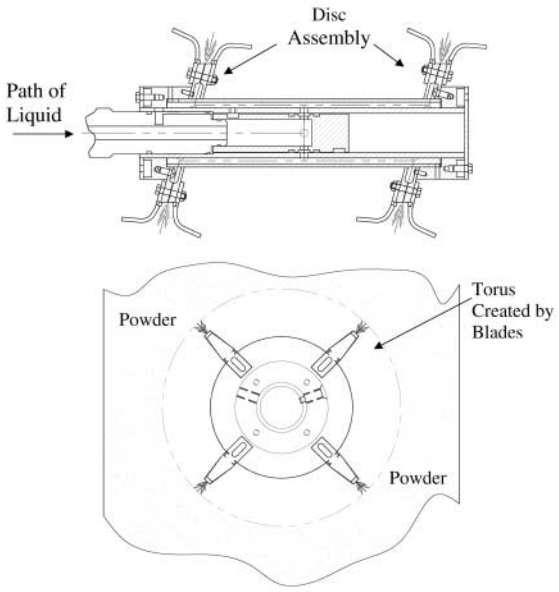

Figure 1. Liquid addition method in LSG.

rapid processing time. A previous article made initial and basic characterizations of wet granulation in this machine using a granulator with a 2-L working volume.[26] This current article expands upon that characterization, addresses scale-up, and proposes methods to determine granulation endpoint.

The research involves using binder strength and agitator bar speed as the factors of interest. The working volume of the research vessel is about 28 times as large as the vessel used in the basic characterization. The earlier characterization used a similar experimental design.

Rigorous scale-up information regarding these machines is rare. Proprietary information is available from the manufacturer but is meant only as a guideline. The proprietary information is based on limited mathematics, some empirical work, and subsequent modification of the scale-up information based on feedback over the years.

The limited scale-up help leaves an experimenter in a quandary in developing the proper processing times to make a comparison to a smaller vessel meaningful. The ultimate processing times chosen for this research are based on the proprietary models.

Developing significant and reproducible scale-up and wet granulation characterization is appropriate because of the pervasiveness of these machines in the pharmaceutical and other industries. Thousands of these LSGs have been sold over the years and are currently in operation primarily as powder mixers.

EXPERIMENTAL

Testing was conducted in a V-shaped, low-shear, tumbling granulator with a working volume of 57 L (Fig. 2). This type of granulator has a fixed shell speed. The shell speed is held constant throughout the size range in which the granulators are manufactured. About 2/3 of the total vessel volume is designated for the material charge, with the remaining 1/3 of the volume utilized as a void volume to ensure proper movement of the material. As Fig. 2 shows, this LSG can be jacketed for use with various heating media. The LSG is vacuum equipped and designed to condense and collect solvent that may be evacuated during a drying step.

The study is designed as a 3^2 factorial experiment with two runs at each condition, yielding a total of 18 tests. The two factors (binder strength and agitator bar speed) are coded as 0 for the low value, 1 for the intermediate value, and 2 for the high value. Each individual test is identifiable by this code. The first digit is an indication of binder strength, the second digit indicates bar speed, and the final digit indicates whether the test is the first or second run at these conditions. For example, 001 means that the test is at low binder strength, low bar speed, and is the first test under these conditions.

Binder strength is determined as a 1%, 2% or 3% (w/w) solids loading of polyvinylpyrrolidone (PVP) K-30 grade on lactose monohydrate powder, USP/NF. Binder is added in an aqueous solution at the proper strength. Bar speed is determined as the peripheral speed at the tip of the blades on the agitator bar. Three speeds, 10.6 m/sec, 14.1 m/sec and 17.6 m/sec are used. The approximate normal tip speed for this particular device is 14.1 m/sec. The other speeds represent values 25% lower and higher than the normal speed. This speed range is readily achievable with an LSG that has a variable speed agitator device. The range encompasses typical speeds encountered in mixing processes. Speeds

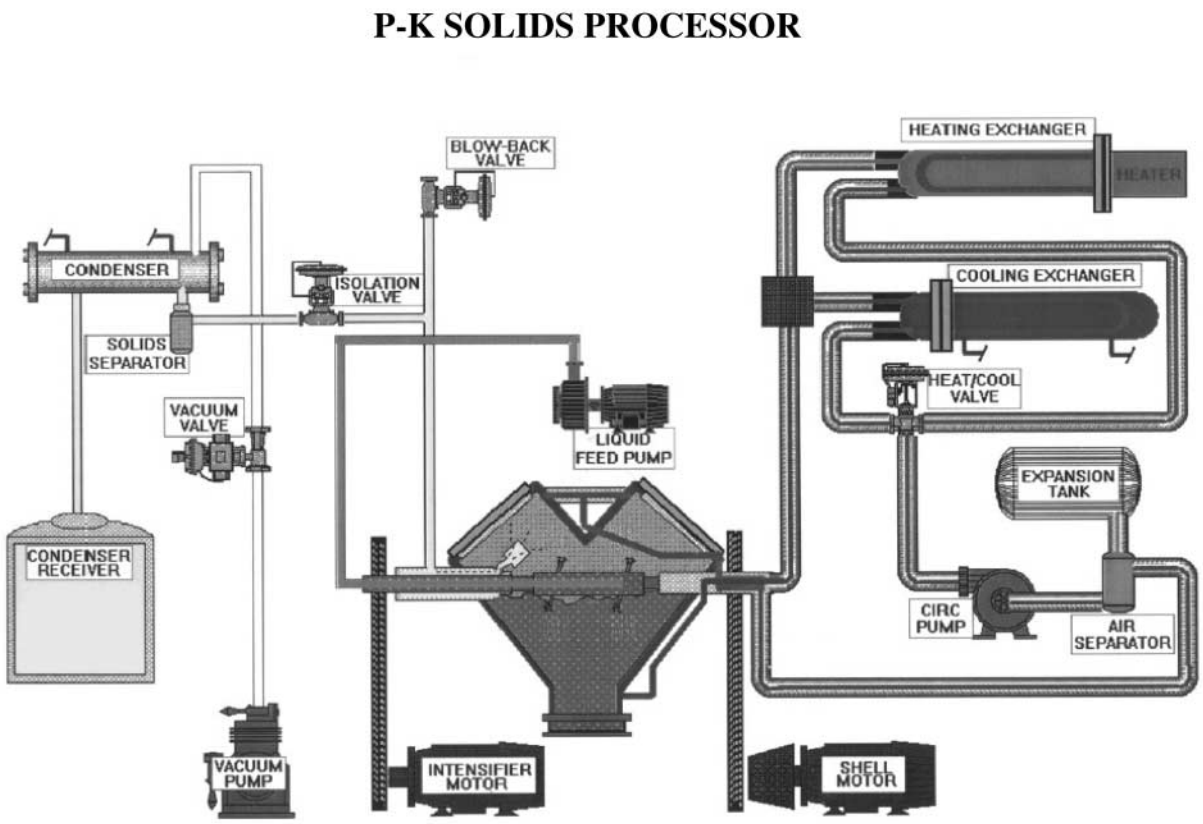

Figure 2. Schematic diagram of a V-type low shear granulator.

beyond the range are permissible but must be evaluated for their influence on wet granulation.

Several response variables are studied through analysis of variance (ANOVA) procedures ($\alpha = 0.05$) including the percentage of dried granules between 150 μm and 1180 μm (the yield fraction), the percentage of granules exceeding 1180 μm (the oversized fraction), the percentage of granules less than 150 μm (the undersized fraction), and the apparent density of the dried granules.

Response variables evaluated through other than statistical methods are the granule morphology by scanning electron microscope (SEM), the peak torque values of the agitator bar during 5-sec intervals by a torque meter, and the cumulative peak torque values during the process by commercial software (SYSTAT® 8.0).

The granulation system (Fig. 3) including the agitator bar, vessel, and torque meter is operated for 600 sec to equilibrate the motor fluids and bearings to ambient conditions.

The granulator is charged with 32 kg of monohydrated lactose powder and the bed temperature is recorded. The initial particle size of the lactose shows 100% less than 250 μm and 85% less than 150 μm.

Binder solution is prepared in the proper strength and the peristaltic pump tubing is primed until the liquid reaches the feed tube on the granulator. The pump setting has been calibrated to deliver 2.743 kg of binder at a rate of 5.0×10^{-3} kg/sec through 2.5×10^{-4} m openings on the periphery of the agitator discs. The binder solution has been prepared so that 2.743 kg contains 1%, 2%, or 3% (w/w) dissolved PVP in relation to the lactose mass. Consequently, the viscosity of the binder solution ranges from about 10 cP at low strength to about 400 cP at high strength.

The granulator vessel motor (vessel peripheral speed fixed at 24 rpm or about 1.5 m/sec) is engaged followed immediately by the agitator bar motor. After an initial 15 sec of running, the torque meter

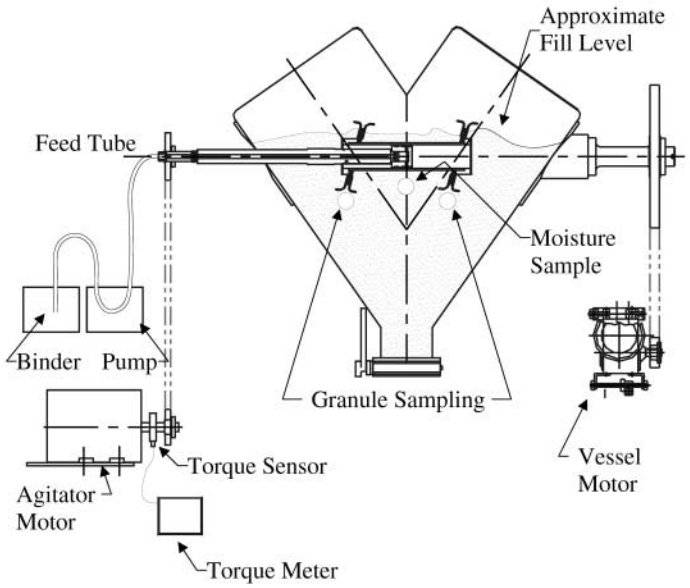

Figure 3. The granulation system.

recordings of the agitator bar begin and continue at 5-sec intervals until the cycle is terminated. Simultaneously, the peristaltic pump is started and continues running until 2.743 kg has been delivered. This period of time that consumes 540 sec is termed the liquid addition (LA) period. The bar and pump continue running for an additional 120 sec to ensure total evacuation of liquid from the bar and aid in total distribution of liquid to the powder mass. This period is termed the post-mix (PM) period. Both the liquid addition rate and the post-mix period were chosen from several combinations evaluated in preliminary testing. Criteria for selection included observation of spray pattern issuing from the disc, ease of handling with the pumping system, evaluation of proprietary scale-up information, and operator experience with similar materials.

The bed temperature of the wet granules is recorded and a moisture sample is collected near the center point of the agitator bar: 300 g samples are collected from the area beneath each disc on the agitator bar. The entire load is discharged to a sampling pan divided into 100 squares. A random number generator is used to select sampling sites for two additional 300 g samples. A site is selected randomly for an additional moisture sample.

Each sample is screened through a #6 mesh (3360 μm) screen and placed in individual drying trays. The granules are dried for 1 hr at 140°C in a convection oven. Upon removal from the oven, the granules are allowed to equilibrate for 15 min, followed by dry screening through the #6 mesh screen. An apparent granule density is recorded for each sample. The dried granules are tapped and sized through 1180 μm, 425 μm, and 150 μm nested screens for 300 sec (Tyler Ro-Tap® TestingSieve Shaker, Model B). The percentage of granules retained on each screen is recorded.

The peak torque value for each 5-sec interval is downloaded from the torque meter and entered into a statistical software program for subsequent analysis.

The granulator is fully disassembled, cleaned, and reassembled for the next run.

RESULTS AND DISCUSSION

The Growth Model and Granule Morphology

The previous growth model proposed for granulation in this LSG favors the development of an equilibrium-type granule that portends an ability to discern an endpoint shortly after liquid addition ends (Fig. 4). The liquid/solid interaction in the LSG is rapid and fresh powder is constantly moving to the zone of liquid influence aided by the movement of the vessel. Diffuse, yield-type granules result. Prolonged agitator use beyond the LA period imparts considerable energy, fragmenting the

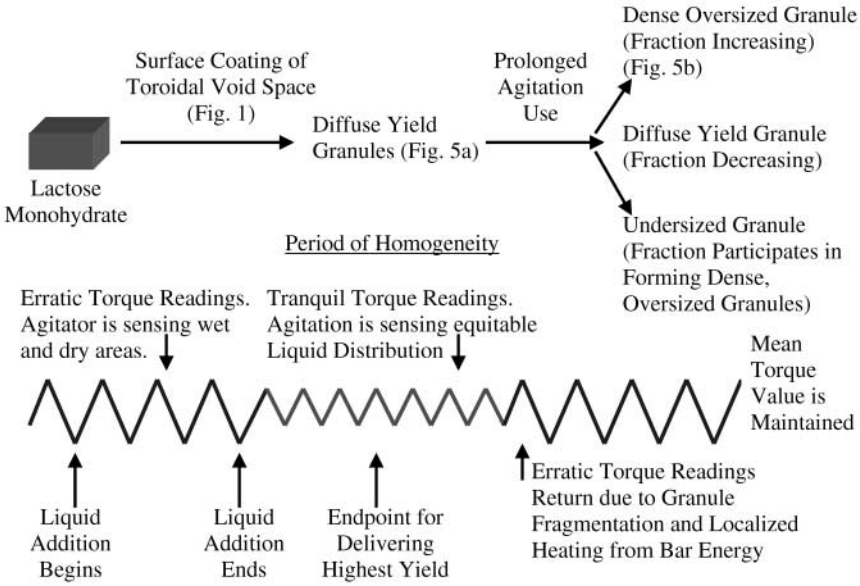

Figure 4. Granulation process in the LSG.

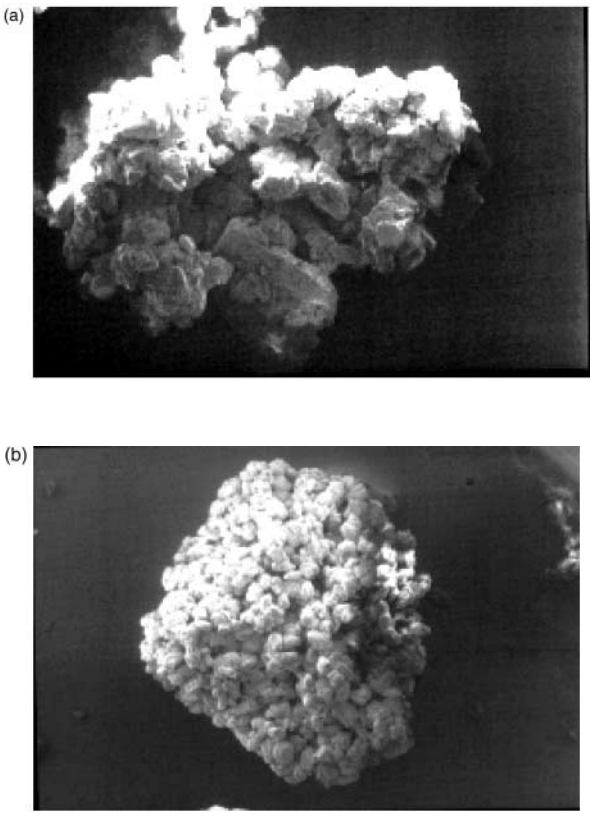

Figure 5. SEM image of (a) yield fraction and (b) oversized fraction.

formed granules and allowing the fragments to participate in forming the dense granules seen in the oversized fraction. Fragments not participating serve to increase the undersized fraction. The granule morphology (Fig. 5) in this testing sequence is similar to the 2l sequence and confirms the basic model shown in Fig. 4. One may note that the yield fraction consists primarily of wet lactose particles that have had surface encounters with other lactose particles. The random nature of the encounters provides asymmetrical granules with substantial open space. By contrast, the oversized fraction has a dense structure resulting from fragments filling the void areas seen in the yield fraction.

Six key components adequately describe the growth sequence (Fig. 6). These include the mass (m) of the individual particles, their corresponding volume (V), the amount of granulating fluid added (L), the instantaneous torque value (T), the cumulative torque to mass ratio ($\Sigma T/m$), and the processing time (t).

The first important event after engaging the motors to start the vessel and agitator bar is that moment when the binder solution encounters a dry particle. As additional liquid enters the system, the mass of lactose divides into a wet and dry fraction. During the liquid addition several events are occurring simultaneously. Granule growth

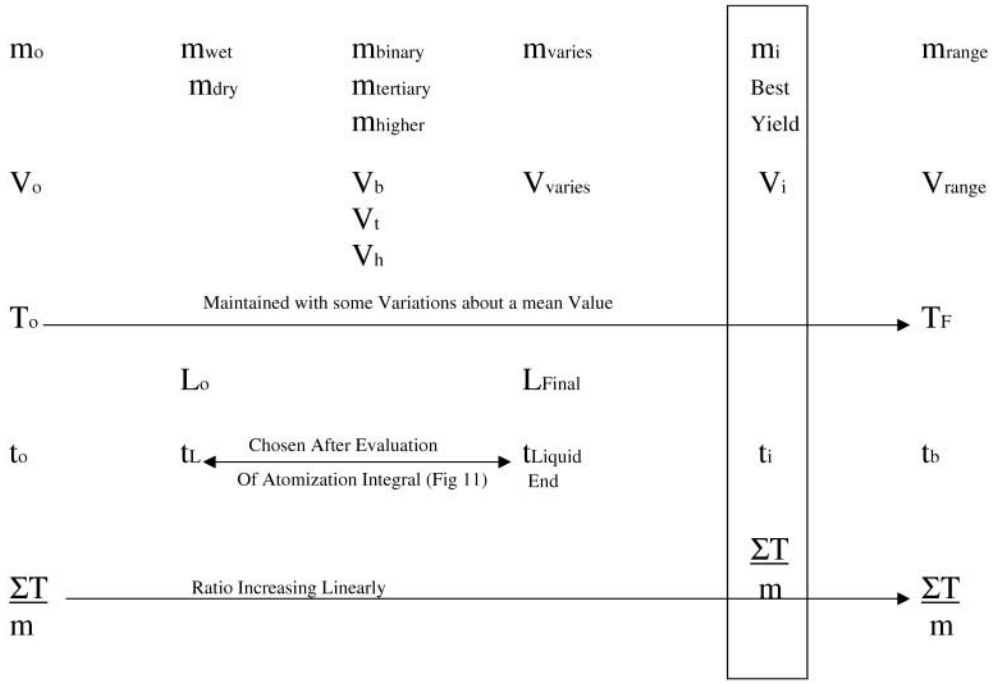

Figure 6. Key components in the growth model.

proceeds as the surface wetting of individual particles and their subsequent movement caused by the action of the vessel and agitator lead to survivable encounters with other particles. The efficiency of the liquid distribution in the LSG minimizes the amount of granulating fluid needed. The low liquid requirement indicates that the granulation process operates in the pendular state as defined by Newitt and Conway-Jones,[27] yielding granules that are primarily held together by liquid bridge bonding and surface tension (i.e., since there is little if any involvement of capillary spaces, there is little involvement of bond strength due to capillary pressure). Fragmentation of formed particles may occur if these granules re-enter the zone of influence of the agitator bar, but the additional liquid they receive allows regrowth with any new encounter.

When liquid addition ends, the granulated powder quickly achieves a state characterized by the equitable distribution of liquid within the powder bed. This period of homogeneity is reflected in the relative tranquility of peak torque readings compared to the wide variation in peak torque values seen during liquid addition (Fig. 4). Continued use of the agitator bar for a length of time beyond liquid addition imparts too much energy to the system. The excessive energy degrades the yield fraction through fragmentation. The fragmentation enhances the oversized fraction by infiltrating and combining with the diffuse granules and producing the dense granules seen in Fig. 5b. The undersized fraction may be enhanced by small pieces that do not participate in forming the dense, oversized granules.

Since the energy input is so critical to the size fraction results, liquid addition is not considered as a singular processing step but as a continuation of energy involvement subsumed within the total running time of the agitator bar. Consequently, the liquid addition time must be chosen as a major portion of the entire process followed by a short post-mix step. Thus a better way of looking at the process is energy involvement during liquid addition and energy involvement post-liquid addition.

The Yield Fraction

The ANOVA results for the size fractions are compared to the characterization work in the 2-L

Table 1

Size Fractions, Density, and Moisture Levels of Granules in Characterization and Scale-Up Testing of an LSG

	% Yield		% Over		% Under		% Moisture		ρ (kg/m^3)	
Test ID	2 L	57 L	2 L	57 L	2 L	57 L	2 L	57 L	2 L	57 L
011	61.2	86.5	35.6	6.4	3.2	7.3	7.6	7.0	364	397
012	65.9	88.5	30.9	7.2	3.2	4.5	7.2	6.7	357	381
111	72.6	87.1	26.8	4.0	0.6	8.9	6.0	5.9	316	396
112	78.9	86.9	20.6	4.8	0.6	8.4	5.9	6.0	349	373
211	87.1	90.0	12.5	1.7	0.4	8.4	5.2	4.8	320	388
212	83.1	90.4	16.0	1.9	0.9	7.7	5.1	4.8	343	389
001	70.0	89.1	29.5	7.4	0.5	3.5	7.4	6.8	327	364
002	73.2	89.7	26.7	7.0	0.1	3.2	7.5	7.0	330	364
101	82.3	90.4	17.3	4.0	0.4	5.6	6.4	6.0	335	384
102	78.7	89.5	21.1	4.2	0.2	6.4	6.3	5.8	335	372
201	91.1	88.3	7.7	1.8	1.3	10.0	5.1	5.1	333	386
202	92.8	90.5	5.4	1.7	1.8	7.9	5.0	4.8	336	394
021	65.4	89.1	34.1	9.5	0.5	1.5	7.5	7.3	336	368
022	62.0	90.2	37.6	7.1	0.4	2.7	7.4	7.1	330	372
121	79.7	92.5	20.1	3.6	0.2	3.9	6.2	6.0	325	381
122	79.3	92.4	20.4	4.2	0.3	3.5	6.0	5.8	332	376
221	90.0	93.9	9.6	1.5	0.4	4.7	5.0	4.9	325	394
222	90.5	93.9	9.1	1.5	0.4	4.6	4.9	5.2	332	396

vessel (Table 1). The results generally affirm the prior work with minor discrepancies explained within the context of the growth model.

The yield fraction increases linearly with binder strength in both the 2-L and 57-L runs (Table 2). Increased binder strength makes it more likely that particle encounters will result in viable granule formation. Increased binder strength makes it less likely that formed granules will be degraded by agitator bar attrition and consequently participate in the oversized and undersized fractions.

Table 2

ANOVA Results for the Yield Fraction

	Significance	
Source of Variance	2 L	57 L
Binder (A)	Yes	Yes
A_{Linear}	Yes	Yes
$A_{Quadratic}$	No	No
Speed (B)	Yes	Yes
B_{Linear}	Yes	Yes
$B_{Quadratic}$	Yes	Yes
Interaction	No	Yes

The yield fraction has a complex relationship with bar speed as evidenced by significant linear and quadratic effects in both the 2-L and 57-L runs. The average yield response as a function of speed in the 2-L sequence shows the best yield at the lowest speed (Fig. 7a). The average yield response also shows the lack of any significant interaction between agitator bar speed and binder strength on the yield fraction.

The average yield response as a function of speed in the 57-L sequence is more complex and reflects the significant interaction between agitator bar speed and binder on the yield fraction (Fig. 7b). The overlap of the curves is a visual indicator of the interaction.

These results can be explained through analysis of the $\Sigma T/m$ ratio and indicate a potential and appropriate endpoint indicator for achieving the best yield. Hancock et al.[28] broached the concept of cumulative energy of mixing (CEM) in dealing with wet granulation in a HSG. The CEM is defined as the integral of the torque vs. time curve. The CEM is an appropriate tool for HSGs where

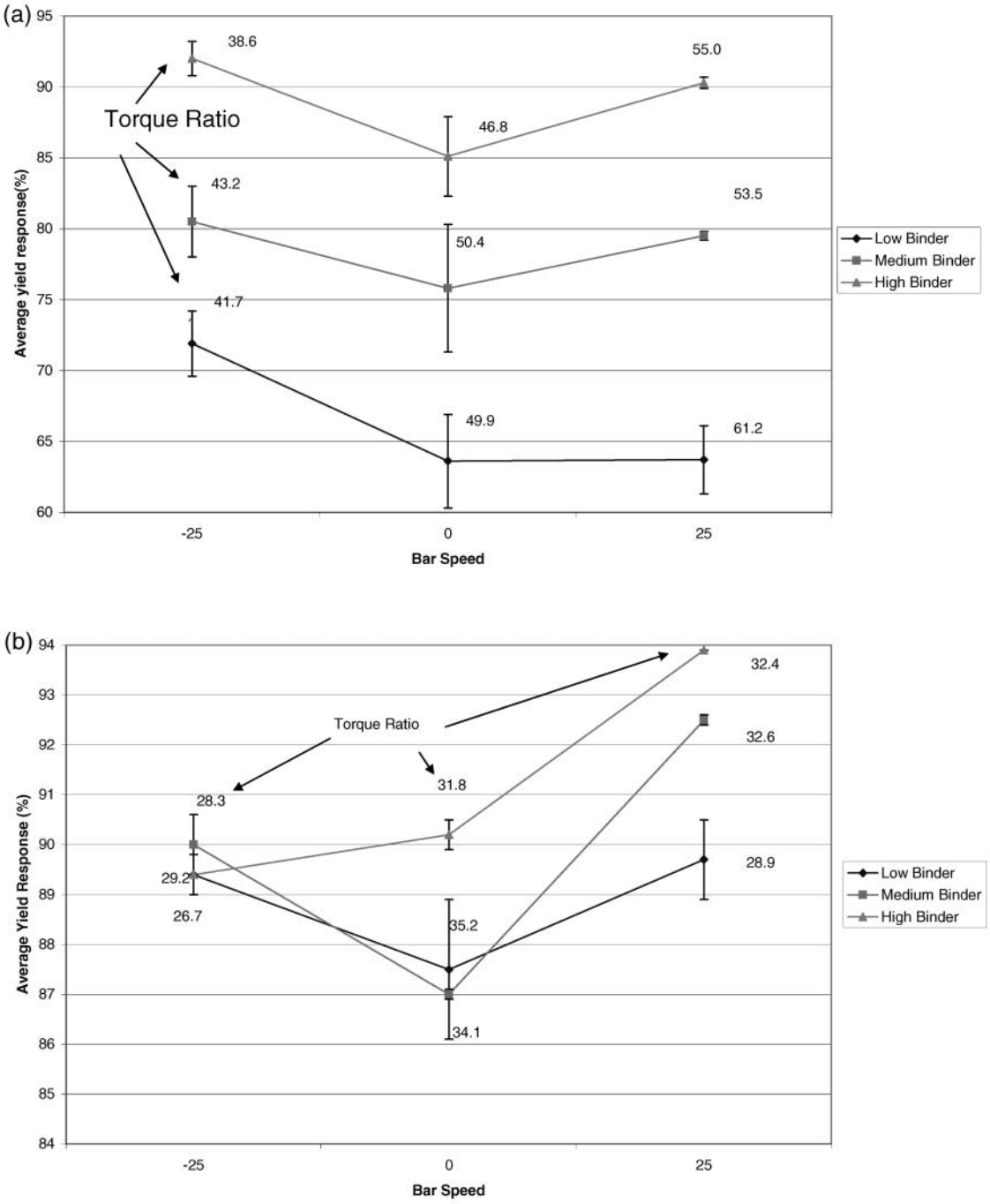

Figure 7. Average yield response as a function of speed in (a) 2-L sequence and (b) 57-L sequence with inserted torque ratios.

the granulation process goes through several stages of increased cohesiveness during the liquid addition phase. The CEM may also be useful for endpoint determination in an LSG. However, one could enhance the energy information by considering the mass of the material undergoing the energy influence. Use of the mass term increases the specificity of the granulation process to the actual material in

Table 3

Cumulative Torque to Mass Ratio (ΣT/m) Average for 2-L and 57-L Testing Sequence

Test ID	Yield	$\Sigma T/m$
22X-57	93.9	32.4
12X-57	92.5	32.6
20X-2	92.0	38.6
22X-2	90.3	55.0
21X-57	90.2	31.8
10X-57	90.0	28.3
02X-57	89.7	28.9
00X-57	89.4	26.7
20X-57	89.4	29.2
01X-57	87.5	35.2
11X-57	87.0	34.1
21X-2	85.1	46.8
10X-2	80.5	43.2
12X-2	79.5	53.5
11X-2	75.8	50.4
00X-2	71.9	41.7
02X-2	63.7	61.2
01X-2	63.6	49.9

the granulator. The $\Sigma T/m$ ratios from Table 3 are inserted in Fig. 7 (error bars represent ± 1 standard deviation). It is logical that at some point in time during the granulation process the best situation of particle size distribution has been achieved for a particular formulation. Relating this instant to a $\Sigma T/m$ value offers the means for endpoint determination and for scale-up to a larger vessel. When the $\Sigma T/m$ ratio is less than ideal for the particular formulation constituents, not enough energy has been imparted to get maximum yield. When the ideal $\Sigma T/m$ ratio is exceeded, too much energy is imparted causing fragments that build into the creation of the dense oversized granules.

This can be seen in Fig. 7a where the lowest $\Sigma T/m$ values are producing the best yields for each binder strength. The lack of interaction between bar speed and binder strength indicates that exceeding the ideal $\Sigma T/m$ ratio goes beyond the point of binder and bar speed interaction on the yield fraction. The agitator bar at this point in time is operating as a chopping device and degrading the yield.

The 57-L runs appear to be operating closer to ideality as defined by the $\Sigma T/m$ ratio. At a ratio of about 32, the three best yields are seen. Values below 32 have lesser yields because insufficient energy has been imparted to effect good distribution of binder. Values greater than 32 have degraded yield fractions because additional energy is causing fragmentation of formed granules and a consequent increase in the dense oversized fraction. Finally, a significant interaction term between binder strength and agitator bar speed is apparent and indicates that the operation closer to an ideal $\Sigma T/m$ ratio maintains this interaction on the yield fraction.

This offers a simple endpoint and scale-up process. One carefully defines the condition that yields the best results for the formulation constituents in the pilot lab, paying particular attention to the $\Sigma T/m$ ratio. The mass of material is adjusted to the scale-up vessel and one seeks that moment in time when the proper $\Sigma T/m$ ratio is recorded. This procedure requires only knowledge of the mass in the vessel and a detector that accumulates the torque values.

The Oversized Fraction

The oversized fraction Table 4 shows an inverse linear relationship to binder strength in both the 2-L and 57-L runs. This is a confirmation of the growth model indicating that the highest binder strength is less likely to suffer fracturing, precluding the generation of fragments that would then participate in forming the densely packed oversized fraction.

The bar speed shows no significant influence on the amount of oversized granules in the 57-L run. This contradicts the significant and complex relationship in the 2-L sequence. This is further indication that the ideal $\Sigma T/m$ ratio has been substantially exceeded in the 2-L sequence, thus allow-

Table 4

ANOVA Results for the Oversized Fraction

	Significance	
Source of Variance	2 L	57 L
Binder (A)	Yes	Yes
A_{Linear}	Yes	Yes
$A_{Quadratic}$	No	No
Speed (B)	Yes	No
B_{Linear}	Yes	No
$B_{Quadratic}$	Yes	No
Interaction	No	No

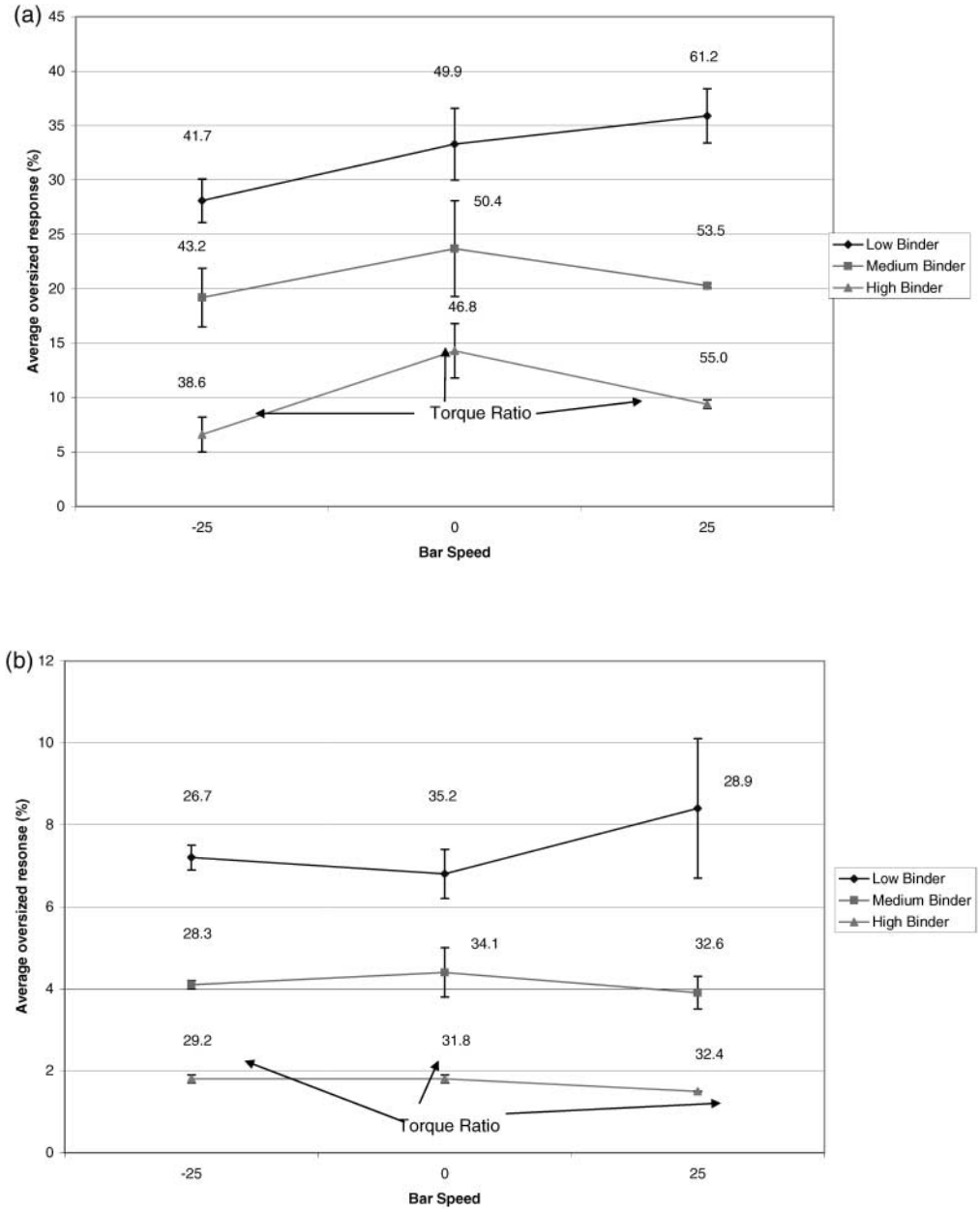

Figure 8. Average oversized response as a function of speed in (a) 2-L sequence and (b) 57-L sequence with inserted torque ratios.

ing fragmentation and growth of the dense oversized fractions. Figure 8a shows that the smallest percentages of oversized granules in the 2-L sequence occur at the lowest $\Sigma T/m$ values for each binder strength. The insignificance of agitator bar speed on the oversized fraction in the 57-L sequence shows that the testing series is operating near the ideal $\Sigma T/m$ ratio. Thus the bar is still acting primarily as a distribution device for the binder liquid. The bar has not yet taken on a major role in fragmentation and consequently the oversized fraction is much less in the 57-L (Fig. 8b) sequence as compared to the 2-L sequence.

The Undersized Fraction

The undersized fraction (Table 5) in both the 2-L and 57-L sequences shows a significant relationship to binder strength. In the 2-L sequence (Fig. 9a) the relationship is complex, while in the 57-L sequence (Fig. 9b) the relationship is linear and increasing. One would expect the opposite results from the proposed growth model since increased binder strength should minimize the tendency toward fragmentation and consequently minimize the undersized fraction. A possible explanation may be that the mobility of the increasingly viscous binder solution is attenuated, preventing participation of some of the original lactose particles at the highest binder strength, thus more undersized are recorded.

The undersized fraction has a significant and complex relationship with bar speed in both testing sequences. The highest speed tends to have the smallest amount of undersized particles. This correlates to the above reasoning about mobility and probably reflects the fact that the greater movement of particles caused by the higher agitator speed is yielding more participation of fragments and original lactose particles.

Table 5

ANOVA Results for the Undersized Fraction

	Significance	
Source of Variance	2 L	57 L
Binder (A)	Yes	Yes
A_{Linear}	Yes	Yes
$A_{Quadratic}$	Yes	No
Speed (B)	Yes	Yes
B_{Linear}	Yes	Yes
$B_{Quadratic}$	Yes	Yes
Interaction	Yes	No

Apparent Density

The apparent density (Table 6) in the 57-L sequence is significantly influenced by the binder strength. This influence is not seen in the 2-L runs. The significance reflects only a slight linear rise in density with respect to the binder strength. The rise is mimicked by the linear rise in the undersized fraction indicating that the increased undersized fraction, in relation to the 2-L sequence, provides a little better packing and consequently a higher apparent density.

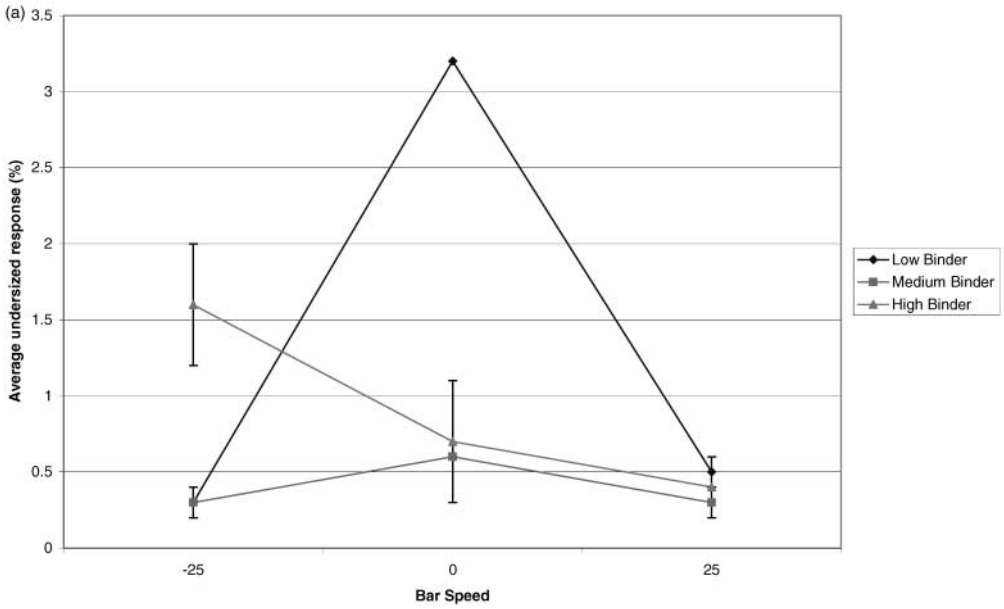

Figure 9. Average undersized response as a function of bar speed in (a) 2-L sequence and (b) 57-L sequence.

(continued)

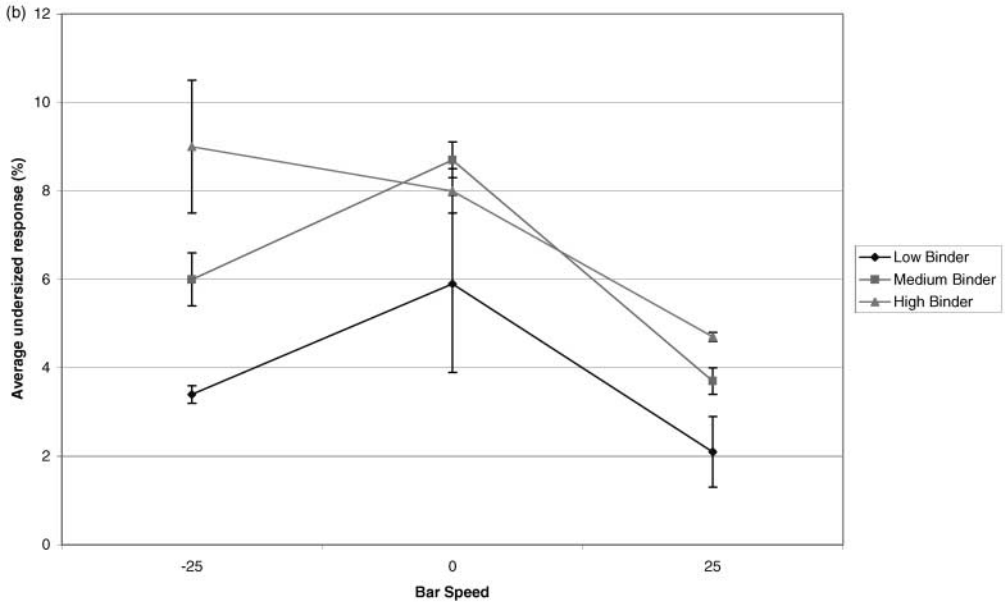

Figure 9. Continued.

Table 6

ANOVA Results for Apparent Density

	Significant	
Source of Variance	2 L	57 L
Binder (A)	No	Yes
Speed (B)	No	No
Interaction	No	No

The bar speed is not a significant contributor to density variance in either the 2-L or 57-L runs.

These results are readily explained within the context of the growth mechanism. Any binder influence on the granulation process is generally felt in how readily the yield fraction may degrade. The structure of the yield fraction however is maintained as the structure of the diffuse granule (Fig. 5a).

The bar speed is influential in the distribution of the liquid. If the liquid has characteristics that allow atomization at the particular bar speed, the yield fraction maintains a common structure and a common apparent density.

The important point remains that despite a 67% increase in bar speed and threefold increase in binder strength in the experimental series, apparent density remains essentially the same. Similar changes in binder strength and agitator speed result in wide ranges of apparent density as reported in several HSG experiments.[29–31] The simplicity and efficiency of this LSG make it an appropriate choice for a wide formulation range.

Scale-Up Considerations

Scale-up of rotating tumbling devices has been addressed as a series of similarity criteria.[32] The criteria include geometric, kinematic, and dynamic similarity. These criteria involve only the rotating vessel and do not take into consideration a high-speed agitator or liquid addition through the agitator device. Each criterion is based on a dimensionless number.

For geometric similarity, two dimensionless numbers are relevant. The first number, J, is the loading fraction taken up by material with respect to the total vessel volume. The second number, r/L_e, is the ratio of rotational radius over the effective length.

The fraction loaded, J, is usually constant for V-type granulators. The nameplate value is the working volume and represents about 2/3 of the

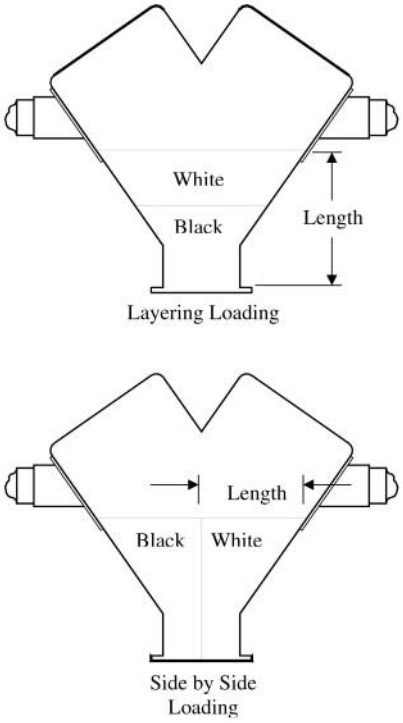

Figure 10. Effective length in vessels related to similarity criteria.[32]

total vessel volume. Thus, the 2-L granulator has a total volume of about 3-L and the 57-L granulator has a total volume of about 85-L. One may note that the volume scale-up is about 28 times but that the mass scale-up is about 45 times for the two testing sequences. This discrepancy results from an anomaly characteristic of the very small granulators. The agitator bar takes up a much larger proportion of the working volume in the smaller vessels and the powder loading must be adjusted to reflect the volume used by the agitator bar. It is important to note that these are volumetric devices that require adequate material loading in order for them to work as designed.

The effective length is a function of the material loading method (Fig. 10). A different effective length is seen for laminar vs. side-by-side loading. In the wet granulation experiment, the only solid formulation constituent is the lactose, so the effective length can be taken as the bed depth at its greatest point. Rotational radius refers to the radius of rotation of the vessel, but since the main energy-imparting device is now the agitator bar, it is appropriate to use the rotating radius of the bar.

Table 7

Assessment of Geometric Similarity Between the 2- and 57-L Granulators

	2 L	57 L
r (m)	4.5×10^{-2}	8.5×10^{-2}
L_e (m)	1.1×10^{-1}	4.7×10^{-1}
r/L_e	4.1×10^{-1}	1.8×10^{-1}

Although consideration has been taken for loading the 2-L and 57-L vessels to the proper working volume, it is apparent that the dimensionless values in Table 7 indicate that geometric similarity has probably not been satisfied in the r/L_e ratio. In addition, it is relatively easy to assign a value to L_e when there are two formulation constituents differing markedly in color or when only a single solid formulation constituent is used. Assigning a value for effective length becomes problematic with more typical formulations containing several constituents.

Kinematic similarity is assessed through the dimensionless number Kt/L_e^2, where K is a mobility coefficient, t is the mixing time, and L_e is the effective length. The mobility coefficient is derived from a semi-logarithmic plot of mix variance vs. time.[32] One must expend a substantial amount of experimental time to evaluate the variance and then construct a plot. Each new formulation requires a new variance vs. time plot.

Dynamic similarity is based on two dimensionless numbers: the Froude number (N^2r/g) and the power number ($P/N^3r^5\rho$). Here, N is the rotational speed (m/sec), r is the rotational radius (m), g is the gravitational constant, P is power (W), and ρ is apparent density (kg/m^3). The power number is considered an independent variable that is related to the Froude number through some function.[32] The function is determined through numerical estimating techniques based on the motor sizes and peripheral speeds of mixers that are already geometrically and kinematically similar.

It is apparent that considerable work is necessary to produce proper scale-up using the similarity criteria. Substantial empirical information must be developed to assess the scale-up functionality of a single formulation.

In practice, geometric similarity is often invoked if the pilot lab and the scale-up vessel are of similar shape (i.e., V-cone to V-cone or double-cone to double-cone). Kinematic similarity is thought to be maintained if both the peripheral speed of the vessel and the agitator bar are kept constant in the pilot lab and scale-up vessel. Dynamic similarity is ultimately related to the motor sizes chosen for the process. The motors are selected through a proprietary scale-up equation derived by the equipment manufacturer. These equations take into consideration appropriate formulation information (intrinsic factors) and appropriate machine information (extrinsic factors) in order to predict a scale-up factor between machine sizes.

The $\Sigma T/m$ ratio offered in this article is a much simpler method that requires only an adequate means to monitor torque input. The method is not dependent on establishing dimensionless numbers that may be difficult to define. It also frees an experimenter from depending upon the equipment manufacturer divulging proprietary scale-up equations.

A further scale-up issue is the liquid addition component of the process. Some manufacturers try to relate scale-up to the liquid evacuation surface of the disc spacing on the agitator bar, but this method tends to overstate the time needed and yields very conservative rates in larger vessels.[33] Generally, the liquid addition time in the larger vessel is a trial and error sequence starting with the predicted conservative time and then shortening the period to a more acceptable production time that yields acceptable results.

The liquid addition method in this LSG is quite elegant in that the agitator bar is multifunctional. It serves as the liquid delivery device, the liquid atomizer and the major bestower of energy to induce granule growth. An analogous situation in a HSG would mean that the impeller or high-speed agitator is serving all these functions.

Liquid in the LSG is fed through a central tube to the interior of the agitator bar where it is directed to each disc assembly (Fig. 1). The speed of the bar literally rips the liquid into tiny droplets. Blades on the periphery of the disc carve out a toroidal void space within the powder bed and liquid droplets moisten the interior of the torus. In a properly loaded vessel, the torus is complete and does not allow any liquid to directly impinge upon the vessel wall. Impingement of free liquid is a primary causative agent for material sticking to the vessel wall.

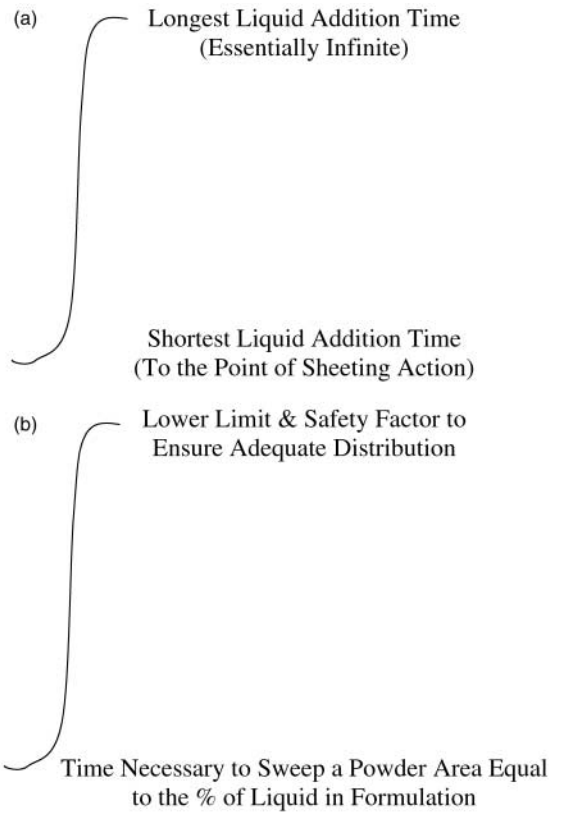

Figure 11. Time integral for liquid atomization: (a) unrestrained and (b) restrained.

Since droplet formation is due to the speed of rotation of the agitator bar, a wide variety of liquid addition rates are possible while still maintaining atomization. Liquid delivery may be as simple as using a gravity feed through a funnel or the liquid may be pumped with a metering device.

Acknowledging the problems regarding liquid addition scale-up, a new and better method would take into consideration extrinsic factors common to the agitator and intrinsic factors common to the formulation constituents.

The liquid addition time frame in the LSG may be thought of in terms of an atomization integral (Fig. 11a). The limits of the integral are quite wide. The upper limit is undefined and depends on how slowly one wishes to deliver the liquid. The admonitions with an extremely slow delivery include excessive process time and particle size degradation.

The lower limit is the point when atomization of the liquid is replaced by sheeting of the liquid. Sheeting occurs when the liquid is pumped rapidly enough to force liquid through the disc periphery, defeating the atomization provided by the rapidly rotating disc.

Determining the appropriate liquid addition rate for a pilot lab vessel and then predicting a suitable scale-up time can be accomplished through definition of three key factors. The useful extrinsic factor is the swept area that the blades carve out in the powder bed. The swept area can be related to an intrinsic factor defining the surface area of the material in the powder bed. For example, the swept area of the blades will eventually equal the amount of surface area contained in the powder. Finally, one should consider the weight percent of the liquid in relation to the powder mass.

It is logical that the lower limit of the integral now is the minimum time it takes to sweep an area of powder equal to the percentage of liquid in the formulation. The upper limit would incorporate some safety factor to ensure adequate distribution. For example, one may wish to exceed the time predicted by the lower limit of the integral by perhaps 10% or 15% (Fig. 11b).

Table 8 offers information on how the atomization integral can be used based on results from the 2-L and 57-L testing sequence. Column 1 identifies an appropriate test grouping. For example, X0X 2-L represents the six test runs that operated at the lowest bar speed in the 2 L study. Grouping according to bar speed is appropriate because the bar speed defines the amount of swept area that the blades travel through during the liquid addition period. Column 2 is the average yield for the test grouping. The yield is directly related to the success of the granulation. It shows the percentage of granules between 150 μm and 1180 μm as a function of bar speed. Column 3 is the ratio of the mass of binder liquid to the mass of powder in the granulator. This is a constant throughout the testing sequence. Although binder strength changes, the mass of binder liquid added and the initial powder in the granulator remain the same. Column 4 is the ratio of the swept surface area described by the agitator bar blades during the liquid addition period over the available surface area of the lactose powder. This column gives one an idea of the amount of powder surface area that may have been exposed to the atomized liquid during binder addition. The best yield is encountered when the Column 4 ratio is near or slightly exceeds the liquid/solid ratio and corresponds to the upper limit of the integral seen if Fig. 11b.

Table 8

Key Components in Assessing the Atomization Integral

Test ID	Average Yield (%)	Liquid/Solid Ratio (%)	Swept Area/Powder Area (%)
X0X 57 L	89.6	8.6	6.9
X1X 57 L	88.2	8.6	9.3
X2X 57 L	92.0	8.6	11.4
X0X 2 L	81.4	8.6	26.3
X1X 2 L	74.8	8.6	34.9
X2X 2 L	77.8	8.6	44.4

Evaluating the Table 8 information yields a useful guide for establishing an appropriate liquid addition time. Short liquid addition times that yield a column 4 ratio less than a column 3 ratio would hamper distribution efficiency. Liquid addition times that provided a comfort zone of perhaps a column 4 ratio exceeding a column 3 ratio by 10% to 30% lie safely within the integral shown in Fig. 11b. Liquid addition times substantially longer than those seen in the atomization integral increase the negative aspects of extended agitator use reflected by degradation of the yield fraction and potential increases in the over- and undersized fractions. Again, consideration of the factors in Table 8 in determining a suitable liquid addition time incorporates both the extrinsic factors of the granulator and the intrinsic factors of the formulation constituents.

Using the proposed method to establish liquid addition times makes scaling-up or scaling-down a straightforward exercise. One considers a coverage rate in the vessel of interest that shows the amount of liquid being distributed per square meter of swept surface area during the liquid addition period. Emulating this coverage rate in a larger or smaller vessel, knowing the amount of liquid needed and the swept area in the vessel of interest yields the scaled-up or scaled-down liquid addition time.

An example from the 2-L and 57-L sequence will clarify the method. Table 9 shows the calculated rates for both testing sequences. Acknowledging the better results in the 57-L testing makes a scale-down example more appropriate. In the X1X series,

Table 9

Swept Area and Coverage Rate During Liquid Addition

Test ID	Swept Area Rate (m^2/sec)	Swept Area During Liquid Addition (m^2)	Coverage Rate (g/m^2)
X0X 57 L	1.8	9.7×10^2	2.8
X1X 57 L	2.4	1.3×10^3	2.1
X2X 57 L	3.0	1.6×10^3	1.7
X0X 2 L	1.1	8.3×10^1	0.72
X1X 2 L	1.5	1.1×10^2	0.54
X2X 2 L	1.8	1.4×10^2	0.43

the coverage rate in the 57-L vessel is 2.1 g/m^2. For similar conditions in the 2-L granulator, the amount of liquid needed is 60 g and the swept area rate for the X1X series is 1.5 m^2/sec. The proper liquid addition time to emulate the 57-L results is shown to be about 20 sec. Using this logic it is abundantly clear that the liquid addition time of 75 sec chosen for the 2-L experimental sequence is substantially longer than necessary.

Endpoint Considerations

Successful endpoint determination in wet granulation has been a problem since the inception of this unit operation as a process step.[34–39] The 2-L testing series showed a reasonably tranquil period shortly after liquid addition ended (Fig. 4). This tranquil period was interpreted as a period of homogeneity reflecting adequate binder distribution and particle growth. The tranquil period ended when excessive use of the agitator bar began to degrade the yield fraction, thereby compromising the homogeneity. The ability to discern a period of tranquility was not repeated in the 57-L testing series. Assessing a period of homogeneity in a larger granulator may be much more difficult because of additional signal noise as compared to that encountered in a well-maintained 2-L table-top granulator.

A better approach to endpoint determination is using the $\Sigma T/m$ ratio. Establishing this ratio in the pilot lab for a test that produces acceptable yield necessitates only instrumentation that can read torque continuously and accumulate the values. This readily ties in with using $\Sigma T/m$ as a means of scaling-up the process. Assessing cumulative torque is particularly appealing to the LSG because the cohesiveness of the powder bed does not noticeably increase during wet granulation. The linear accumulation of torque is seen in the 2-L test and repeated in the 57-L test. Unlike an HSG that requires copious granulating fluid and shows a characteristic curve reflecting the increased torque,[40] this LSG requires minimal granulation fluid. The low requirement for binder liquid is advantageous in reducing liquid addition times and subsequent drying times.

SUMMARY

The 57-L scale-up sequence confirms the basic results seen in the 2-L characterization of wet granulation in an LSG. This granulating method provides a rapid process, is amenable to wide formulation variations, and offers easy methods to discern endpoint and scale-up. This granulator type equipped with a heating and vacuum package is an excellent choice for single-pot processing, incorporating dry mixing, wet granulation, drying, and lubrication of a tablet formulation without removal from the vessel.

REFERENCES

1. *Handbook of Pharmaceutical Granulation Technology*, Parikh, D.M., Ed.; Marcel Dekker: New York, 1997.
2. Lacey, P.M.C. The Mixing of Solid Particles. Trans. Inst. Chem. Eng. **1943**, *21*, 53–59.
3. Kristensen, H.G. Agglomeration of Powders. Acta Pharm. Suec. **1988**, *25*, 187–204.
4. Carstensen, J.T.; Lai, T.; Flickner, D.W.; Huber, H.E.; Zoglio, M.A. Physical Aspects of Wet Granulation I: Distribution Kinetics of Water. J. Pharm. Sci. **1976**, *65* (7), 992–997.
5. Kristensen, H.G.; Schaefer, T. Granulation—A Review on Pharmaceutical Wet Granulation. Drug Dev. Ind. Pharm. **1987**, *13* (4&5), 803–872.
6. Stamm, A.; Paris, L. Influence of Technological Factors on the Optimal Granulation Liquid Requirement Measured by Power Consumption. Drug Dev. Ind. Pharm. **1985**, *11* (2&3), 333–360.
7. Pilpel, N. Granulation of Pharmaceuticals. Chem. Proc. Eng. **1969**, *July*.
8. Parker, M.D.; York, P.; Rowe, R.C. Binder–Substrate Interaction in Wet Granulation. 1. The Effect of Binder Characteristics. Int. J. Pharm. **1990**, *64*, 207–216.

9. Rowe, R.C. Binder–Substrate Interactions in Granulation: A Theoretical Approach Based on Surface Free Energy Polarity. Int. J. Pharm. **1989**, *52*, 149–154.
10. Schaefer, T. Equipment for Wet Granulation. Acta Pharm. Suec. **1988**, *25*, 205–228.
11. Titley, P.C. Agglomeration and Granulation of Powders, Processing and Manufacturing Practice. Acta Pharm. Suec. **1988**, *25*, 267–280.
12. Zoglio, M.A.; Huber, H.E.; Koehne, G.; Chan, P.L.; Carstensen, J.T. Physical Aspects of Wet Granulation II: Factors Involved in Prolonged and Excessive Mixing. J. Pharm. Sci. **1976**, *65* (8), 1205–1208.
13. Zoglio, M.A.; Carstensen, J.T. Physical Aspects of Wet Granulation III: Effect of Wet Granulation on Granule Porosity. Drug Dev. Ind. Pharm. **1983**, *9* (8), 1417–1434.
14. Ghanta, S.R.; Srinivas, R.; Rhodes, C.T. Use of Mixer-Torque Measurements as an Aid to Optimizing Wet Granulation Process. Drug Dev. Ind. Pharm. **1984**, *10*(2), 305–311.
15. Alleva, D.S.; Schwartz, J.B. Granulation Rheology I: Equipment Design and Preliminary Testing. Drug Dev. Ind. Pharm. **1986**, *12* (4), 471–487.
16. Remon, J.P.; Schwartz, J.B. Effect of Raw Materials and Processing on the Quality of Granules Prepared from Microcrystalline Cellulose–Lactose Mixtures. Drug Dev. Ind. Pharm. **1987**, *13* (1), 1–14.
17. Parker, M.D.; York, P.; Rowe, R.C. Binder–Substrate Interactions in Wet Granulation. 2. The Effect of Binder Molecular Weight. Int. J. Pharm. **1991**, *72*, 243–249.
18. Vojnovic, D.; Selenati, P.; Rubessa, F.; Moneghini, M. Wet Granulation in a Small Scale High Shear Mixer. Drug Dev. Ind. Pharm. **1992**, *18* (9), 961–972.
19. Corvari, V.; Fry, W.C.; Seibert, W.L.; Augsberger, L. Instrumentation of a High Shear Mixer: Evaluation and Comparison of a New Capacitive Sensor, a Watt Meter and a Strain-Gage Torque Sensor for Wet Granulation Monitoring. Pharm. Res. **1992**, *9* (12), 1525–1533.
20. Kopcha, M.; Roland, E.; Bubb, G.; Vadino, W.A. Instrumentation of a Vertical High Shear/Mixer Granulator to Monitor the Granulation Operation. Drug Dev. Ind. Pharm. **1992**, *18* (18), 1945–1968.
21. Vojnovic, D.; Moneghini, M.; Rubessa, F. Simultaneous Optimization of Several Response Variables in a Granulation Process. Drug Dev. Ind. Pharm. **1993**, *19* (12), 1479–1496.
22. Wehrle, P.; Nobelis, Ph.; Cuine, A.; Stamm, A.; Response Surface Methodology: An Interesting Statistical Tool for Process Optimization and Validation: Example of Wet Granulation in a High Shear Mixer. Drug Dev. Ind. Pharm. **1993**, *19*(13), 1637–1653.
23. Vojnovic, D.; Moneghini, M.; Rubessa, F. Optimization of Granulation in a High Shear Mixer by Mixture Design. Drug Dev. Ind. Pharm. **1994**, *20* (6), 1035–1047.
24. Sheskey, P.J.; Williams, D.M. Comparison of Low-Shear and High-Shear Wet Granulation Techniques and the Influence of Percent Water Addition in the Preparation of a Controlled-Release Matrix Tablet Containing HPMC and a High-Dose, Highly Water-Soluble Drug. Pharm. Technol. *20* (3), 80–91.
25. Nouh, A.T.I. The Effect of Variations in Concentration and Type of Binder on the Physical Characteristics of Sulfadiazine Tablets and Granulation Prepared by Wet and Fluidized-Bed Granulation Method. Pharm. Ind. **1986**, *48* (6).
26. Chirkot, T.S. Characterization of a Pharmaceutical Wet Granulation Process in a V-Type Granulator. Pharm. Eng. **1999**, *19* (4), 50–61.
27. Newitt, D.; Conway-Jones, J. Trans. Instr. Chem. Engrs. **1958**, *36*, 422.
28. Hancock, B.C.; York, P.; Rowe, R.C.; Parker, M.D.; Characterization of Wet Masses Using a Mixer-Torque Rheometer: 1. Effect of Instrument Geometry. Int. J. Pharm. **1991**, *76*, 239–245.
29. Lipps, D.M.; Sakr, A.M. Characterization of Wet Granulation Process Parameters Using Response Surface Methodology. 1. Top Spray Fluidized Bed. J. Pharm. Sci. **1994**, *83* (7), 937–947.
30. Lindberg, N.O.; Jonsson, C. The Granulation of Lactose and Starch in a Recording High-Shear Mixer, Diosna P25. Drug Dev. Ind. Pharm. **1985**, *11* (2&3), 387–403.
31. Paris, L.; Stamm, A. Optimal Massing Liquid Volume Determination by Energy Consumption Measurements: Study of the Influence of Some Physical Properties of Solvents and Products Used. Drug Dev. Ind. Pharm. **1985**, *11* (2&3), 361–386.
32. Wang, R.H.; Fan, L.T. Methods for Scaling-Up Tumble Blenders. Chem. Eng. **1974**, May, 88–94.
33. Patterson-Kelley Proprietary Documents; Patterson-Kelley Co., East Stroudsburg, PA.
34. Kay, D.; Record, P.C. Automatic Wet Granulation End-Point Control System. Manuf. Chem. Aerosol News **1978**, *Sept*, 45–46.
35. Fry, W.C.; Stagner, W.C.; Wichman, K.C. Computer-Interfaced Capacitive Sensor for Monitoring the Granulation Process. J. Pharm. Sci. **1984**, *73* (3), 420–421.
36. Werani, J. Production Experience with End Point Control. Acta Pharm. Suec. **1988**, *25*, 247–266.
37. Cliff, M.J. Granulation Endpoint and Automated Process Control of Mixer-Granulators: Part I. Pharm. Technol. **1990**, *April*, 112–132.
38. Cliff, M.J. Granulation Endpoint and AutomatedProcess Control of Mixer-Granulators: Part II. Pharm. Technol. Int. **1990**, *Feb*, 18–22.

39. Watano, S.; Terashita, K.; Miyanami, K.; Determination of an End-Point with a Complex Granulation Applying Infrared Moisture Sensor. Chem. Pharm. Bull. **1991**, *39* (*4*), 1013–1017.

40. Leuenberger, H.; Bier, H.-P.; Sucker, H.B. Theory of Granulating Liquid Requirement in the Conventional Granulating Process. Pharm. Technol. **1987**, *June*, 76–80.